PROCEEDINGS OF SCIENCE

Study of the neutrino-oxygen neutral-current quasielastic cross section using atmospheric neutrinos in the SK-Gd experiment

Seiya Sakai[a,*] **on behalf of the Super-Kamiokande Collaboration**

[a] *Department of Physics, Okayama University, Okayama, Okayama 700-8530, Japan*

E-mail: sakaipartphys@s.okayama-u.ac.jp

The atmospheric neutrino-oxygen neutral-current quasielasatic (NCQE) reactions are one of the main background in the search for supernova relic neutrinos. Here, we report the first measurement of the atmospheric neutrino-oxygen NCQE cross section in the Super-Kamiokande Gadolinium (SK-Gd) experiment using 552.2 days of full SK-VI data. The measured NCQE cross section is $0.74 \pm 0.22(\text{stat.})\,^{+0.86}_{-0.16}(\text{syst.}) \times 10^{-38}$ cm^2, which is consistent with the theoretical NCQE cross section and the previous study in SK within the range of the uncertainty. Furthermore, we established the verification method for nucleon-nucleus interaction models using atmospheric neutrino events. We performed the verification using the Bertini Cascade model (BERT), the Binary Cascade model (BIC) and the Liège Intranuclear Cascade model (INCL++). As a result, we suggested that BIC and INCL++ are closer to the observed data.

38th International Cosmic Ray Conference (ICRC2023)
26 July - 3 August, 2023
Nagoya, Japan

*Speaker

PoS(ICRC2023)1088

1. Introduction

Neutrinos emitted from all past core-collapse supernovae form the integrated flux, called the supernova relic neutrinos (SRN). Detecting the SRN would enable us to understand the supernova mechanism as well as the star formation history. Currently, we are aiming to the world's first observation of the SRN in the Super-Kamiokande Gadolinium (SK-Gd) experiment [1]. In the SRN search, we look for the inverse beta decay (IBD) events by electron-antineutrinos ($\overline{\nu}_e + p \rightarrow e^+ + n$). The positron emits Cherenkov photons immediately, while the neutron is captured on Gd and total about 8 MeV gamma-rays are emitted. By detecting the positron-like signal (prompt signal) and the neutron signal (delayed signal), we can remove large number of backgrounds that does not contain neutrons. However, backgrounds that contain neutrons cannot be removed and remains.

One of the main backgrounds in the SRN search is caused by the atmospheric neutrino-oxygen neutral-current quasielastic (NCQE) reactions. NCQE reactions can be expressed as

$$\begin{aligned} \nu(\bar{\nu}) + {}^{16}\mathrm{O} &\rightarrow \nu(\bar{\nu}) + {}^{15}\mathrm{O}^* + \mathrm{n}, \\ \nu(\bar{\nu}) + {}^{16}\mathrm{O} &\rightarrow \nu(\bar{\nu}) + {}^{15}\mathrm{N}^* + \mathrm{p}, \end{aligned} \tag{1}$$

where the atmospheric neutrino knocks out a nucleon of the oxygen nucleus and the residual nucleus emits de-excitation gamma-ray. When a neutron is knocked out, the neutron is captured on Gd and gamma-rays are emitted. The combination of de-excitation gamma-ray and neutron mimics the IBD events, thus it is hard to identify that. Therefore, it is essential to estimate the NCQE events precisely for the SRN discovery.

To estimate the NCQE events precisely, we must understand the behavior of neutrons in water. In IBD events, the outgoing neutron has at most a few MeV. On the other hand, in NCQE events, the knocked out neutron has hundreds of MeV, thus the neutron can knock out other nucleon of the oxygen nucleus. As a result, additionally de-excitation gamma-rays and neutrons are generated. We must understand the energy of each de-excitation gamma-ray and the number of de-excitation gamma-rays and neutrons for the precise NCQE estimation. Currently, in the SRN search, systematic uncertainty of NCQE events is 68% below 15.5 MeV and 82% above 15.5 MeV of reconstructed prompt energy [2]. This large uncertainty mainly comes from energy spectrum shape and neutron multiplicity, which are strongly related to nucleon-nucleus (secondary) interactions. To achieve the SRN discovery, it is essential to understand the secondary interactions and reduce the uncertainty. So far, the GEANT3-based SK detector simulation have been used in the physics analyses, thus the obsolete secondary interaction model based on the Bertini Cascade model (BERT) was the only choice. Therefore, we performed the detector simulation using the newly developed Geant4-based simulator so that we can compare the observed data with the latest secondary interaction models. Here, we report the reproducibility of the observed data in each secondary interaction model using atmospheric neutrino events. In addition, we report the first measurement of the neutrino-oxygen NCQE cross section using atmospheric neutrino events in the SK-Gd experiment and the consistency of the measured NCQE cross section with previous study (pure water phase) [3].

2. Super-Kamiokande

SK [4] is the large water Cherenkov detector located in Kamioka, Gifu, Japan. SK is in 1,000 m underground, which is comparable to 2,700 m water equivalent, thus the cosmic ray muons is reduced by a factor of 10^5 compared to ground surface. The detector consists of the stainless-steel cylindrical water tank with a diameter of 39.3 m and a height of 41.4 m and 50 kilotons ultrapure water. The water tank is separated into the inner detector (ID) and the outer detector (OD) optically. ID has 11,129 20-inch PMTs to reconstruct the energy, generated position, direction and the kind of the charged particles. On the other hand, OD has 1,885 8-inch PMTs to veto cosmic ray muons. Radioactive backgrounds are rich near the detector wall, thus events 2 m away from the ID wall is used in the analyses, resulting in the fiducial volume of 22.5 kilotons.

SK started its observation in April 1996, and so far, the observation phase is categorized into seven (from SK-I to SK-VII). In September 2008, the data acquisition system was renewed, and SK-IV phase started. The renewal of the system allows us to open the data acquisition time window until 535 μs from the trigger timing and enabled to search neutron signals. But until SK-V, the neutron signal was a 2.2 MeV gamma-ray from neutron capture on free proton and the neutron tagging efficiency was low. To increase the efficiency, we loaded 0.011% of Gd in SK and SK-VI (SK-Gd) phase started in July 2020. In June 2022, Gd concentration became 0.03% and we continue the observation as SK-VII phase.

The previous NCQE cross section measurement in SK was performed using 2,778 days of SK-IV data from October 2008 to October 2017 [3]. This measurement uses 552.2 days of SK-VI data from August 2020 to June 2022, where the data set is the same as the SRN search in SK-VI [2].

3. Simulation

The atmospheric neutrino flux at the SK is predicted using the HKKM11 model [5], which shows good agreement with the observation in the SK pure water phase [6]. Therefore, we take the HKKM11 model as the input atmospheric neutrino flux model, which is used in previous study [3].

Neutrino interactions are simulated using NEUT [7] (version 5.4.0.1). The NCQE cross section on oxygen is based on the Ankowski model [8]. The state of oxygen nucleus after neutrino-nucleus (primary) interaction is selected based on the probabilities computed in Ref. [8]. There are four states, $(p_{1/2})^{-1}$, $(p_{3/2})^{-1}$, $(s_{1/2})^{-1}$ and *others*. The production probability of each state is 0.1580, 0.3515, 0.1055 and 0.3850, respectively. $(p_{1/2})^{-1}$ state is the ground state of ^{15}O or ^{15}N, thus no gamma-ray is emitted. While mainly 6.18 MeV or 6.32 MeV gamma-ray is emitted from $(p_{3/2})^{-1}$ state of ^{15}O or ^{15}N. In the case of $(s_{1/2})^{-1}$ state, nucleon in addition to gamma-rays are emitted because its excitation energy is higher. *others* state includes all other modes that are not included in $(p_{1/2})^{-1}$, $(p_{3/2})^{-1}$ and $(s_{1/2})^{-1}$ state. There is no data nor theoretical predictions of modes covered by *others* state, thus *others* state is integrated into $(s_{1/2})^{-1}$ state in default.

The particle transportation as well as detector response are simulated by Geant4-based simulation package (version 10.05.p01). As the secondary interaction model, BERT (`FTFP_BERT_HP` physics list) is used in the NCQE cross section measurement. In the verification of secondary interaction models, in addition to BERT, the Binary Cascade model (BIC, `QGSP_BIC_HP` physics list) and the Liège Intranuclear Cascade model (INCL++, `INCLXX_HP` physics list) are used.

4. Event reconstruction and selection

We follow the event reconstruction and selection of the SRN search in SK-VI [2], except for the reconstructed Cherenkov angle for prompt signal (θ_{C}) and the number of delayed signals per event (N_{delayed}). In IBD event, only one positron and one neutron are emitted. Therefore, θ_{C} and N_{delayed} tend to be about 42 degrees and one, respectively. On the other hand, in NCQE event, multiple gamma-rays and multiple neutrons are easy to be emitted. Therefore, θ_{C} and N_{delayed} tend to be greater than 42 degrees and greater or equal to one, respectively. In this study, we select the events that θ_{C} is greater than 50 degrees and N_{delayed} is greater or equal to one so that NCQE events are dominant. Furthermore, we select the events that the reconstructed prompt energy is between 7.5 MeV and 29.5 MeV, which is the signal energy region of the SRN search in SK-VI [2]. The cut criteria of θ_{C}, the reconstructed prompt energy and N_{delayed} are the same as the previous study [3].

5. Results

5.1 Measured NCQE cross section

After applying all event selections to 552.2 days of SK-VI data, 38 events were remained. In previous study [3], 117 events were remained after applying all event selections to 2,778 days of SK-IV data. This means that we achieved about 1.6 times signal efficiency larger than the previous study [3]. The expected events include NCQE events, atmospheric neutrino NC non-QE events, atmospheric neutrino charged-current (CC) events, spallation events by cosmic ray muons, reactor neutrino events and accidental coincidence events. Accidental coincidence events are the pairs of prompt signal and misidentified delayed signal caused by PMT noise hits and radioactive backgrounds. The events are estimated by

$$N^{\mathrm{exp}}_{\mathrm{Accidental}} = \varepsilon_{\mathrm{mis}} \times N^{\mathrm{obs}}_{\mathrm{pre\text{-}ntag}}, \tag{2}$$

where $\varepsilon_{\mathrm{mis}}$ ($= 2.8 \times 10^{-4}$) is the neutron misidentification rate [2] and $N^{\mathrm{obs}}_{\mathrm{pre\text{-}ntag}}$ is the observed number of events after applying all event selections except for N_{delayed} cut. The expected number of these events and event fraction are summarized in Table 1. After applying all event selections, NCQE events are dominant (62.5%), and NC non-QE events are sub-dominant (28.9%). The flux-averaged theoretical NCQE cross section is

$$\langle \sigma^{\mathrm{theory}}_{\mathrm{NCQE}} \rangle = \frac{\int^{10\ \mathrm{GeV}}_{160\ \mathrm{MeV}} \sum_{i=\nu,\bar{\nu}} \phi_i(E) \times \sigma_i(E)^{\mathrm{theory}}_{\mathrm{NCQE}} dE}{\int^{10\ \mathrm{GeV}}_{160\ \mathrm{MeV}} \sum_{i=\nu,\bar{\nu}} \phi_i(E) dE} = 1.02 \times 10^{-38}\ \mathrm{cm}^2, \tag{3}$$

where $\phi_i(E)$ is the atmospheric neutrino flux at neutrino energy E and $\sigma_i(E)$ is the theoretical NCQE cross section. The integral is performed between 160 MeV and 10 GeV because the NCQE cross section is small below 160 MeV and the atmospheric neutrino flux is small above 10 GeV. The energy cutoff is evaluated as a systematic uncertainty. The measured NCQE cross section is

$$\langle \sigma^{\mathrm{measured}}_{\mathrm{NCQE}} \rangle = \frac{N^{\mathrm{obs}} - N^{\mathrm{exp}}_{\mathrm{Non\text{-}NCQE}}}{N^{\mathrm{exp}}_{\mathrm{NCQE}}} \times \langle \sigma^{\mathrm{theory}}_{\mathrm{NCQE}} \rangle = 0.74 \pm 0.22(\mathrm{stat.}) \times 10^{-38}\ \mathrm{cm}^2, \tag{4}$$

Components	Events	Fraction
Total	45.8991	100.0%
NCQE	28.7071	62.5%
NC non-QE	13.2721	28.9%
CC	1.4177	3.1%
Spallation	0.8879	1.9%
Reactor neutrino	0.0619	0.1%
Accidental coincidence	1.5524	3.4%

Table 1: The expected number of events and event fraction.

	NCQE	NC non-QE	CC
Neutrino flux	18.0%	18.0%	18.0%
Neutrino/antineutrino ratio	5.0%	5.0%	-
Cross section	-	18.0%	24.0%
Primary interaction	+1.9%/−9.8%	−2.6%	+7.3%/−10.4%
Secondary interaction	−32.1%	−22.9%	−20.9%
Energy cutoff	−1.6%	−1.5%	−18.9%
Data reduction	1.4%	1.4%	1.4%
Neutron tagging	6.4%	6.4%	6.4%
	Spallation	Reactor neutrino	Accidental coincidence
Systematic uncertainty	60.0%	100.0%	4.6%

Table 2: Systematic uncertainties of the expected events.

where N^{obs} is the observed number of events, $N^{\text{exp}}_{\text{NCQE}}$ is the expected number of NCQE events and $N^{\text{exp}}_{\text{Non-NCQE}}$ is the expected number of Non-NCQE events including NC non-QE, CC, spallation, reactor neutrino and accidental coincidence.

5.2 Systematic uncertainties

Systematic uncertainties of the expected events are summarized in Table 2. The atmospheric neutrino flux uncertainty and the atmospheric neutrino/antineutrino ratio uncertainty are the same as previous study in SK [3]. The cross section uncertainty is the same as previous study in T2K [9]. As for the estimation of primary interaction uncertainty, we referred to the estimation method of previous study in T2K [10]. The secondary interaction uncertainty is taken to be the maximum difference from BERT to BIC or INCL++. The verification of secondary interaction models is described in Sec. 5.3. The energy cutoff uncertainty is taken to be the sum in quadrature of the "$E > 160$ MeV" case and "$E < 10$ GeV" case, where E is the energy of atmospheric neutrinos used in event estimation. The expected number of events decreases by the energy cutoff, thus only negative direction is considered. The data reduction uncertainty is 1.4% [11]. The neutron tagging efficiency is 6.4%, which was estimated using Americium-241/Beryllium-9 radioactive source [2]. Systematic uncertainties of spallation events and reactor neutrino events are 60% and

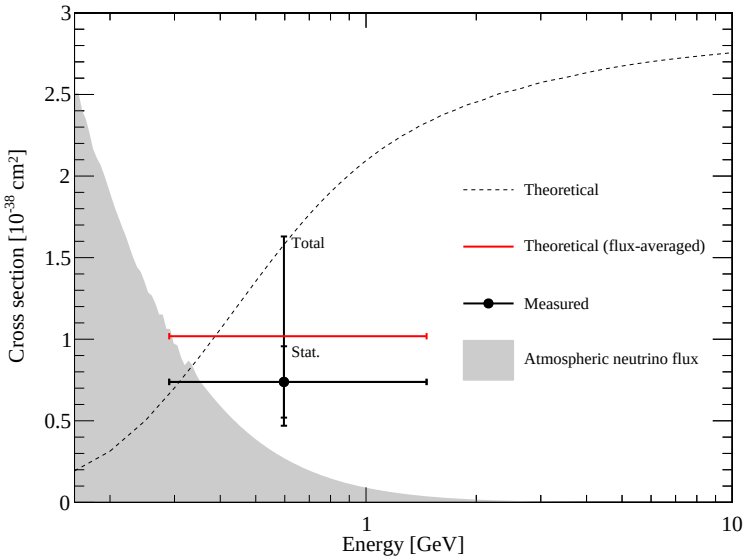

Figure 1: The measured NCQE cross section, the theoretical NCQE cross section and the atmospheric neutrino flux predicted using the HKKM11 model. The atmospheric neutrino flux is shown with an arbitrary normalization. Vertical bars show the statistical uncertainty (short bar) and the quadratic sum of statistical and systematic uncertainties (long bar). Horizontal bars show the 1σ from the mean (0.60 GeV) of the theoretical NCQE cross section multiplied by the atmospheric neutrino flux.

100%, respectively [2]. However, the effect to the measured NCQE cross section calculation is small because the event fraction of spallation events and reactor neutrino events is small as shown in Table 1. Systematic uncertainty of accidental coincidence events is taken by considering the systematic uncertainty of ε_{mis} and the statistical uncertainty of $N^{\text{obs}}_{\text{pre-ntag}}$, which are shown in Eq. (2).

Systematic uncertainty of the measured NCQE cross section is estimated by performing toy-MC considering the systematic uncertainties in Table 2. As a result, the 1σ confidence level region becomes $[0.58, 1.60] \times 10^{-38}$ cm^2, and the measured NCQE cross section is determined as

$$\langle \sigma^{\text{measured}}_{\text{NCQE}} \rangle = 0.74 \pm 0.22(\text{stat.}) \, ^{+0.86}_{-0.16}(\text{syst.}) \times 10^{-38} \, \text{cm}^2. \tag{5}$$

The measured NCQE cross section, the theoretical NCQE cross section and the atmospheric neutrino flux predicted using the HKKM11 model are shown in Fig. 1. The measured NCQE cross section is consistent with the flux-averaged theoretical NCQE cross section within the range of the uncertainty. Furthermore, the measured NCQE cross section is consistent with the previous study ($1.01 \pm 0.17(\text{stat.}) \, ^{+0.78}_{-0.30}(\text{syst.}) \times 10^{-38}$ cm^2) [3]. From these results, we can say that the performance of the SK-Gd experiment is well.

5.3 Secondary interaction models

Thanks to the development of the Geant4-based simulation package, we can use various secondary interaction models and chase the property of each model. Here we show the change of the distributions of θ_{C}, the reconstructed prompt energy and N_{delayed} by the difference of secondary interaction models. Furthermore, we discuss which secondary interaction model is more appropriate by comparing with the observed data.

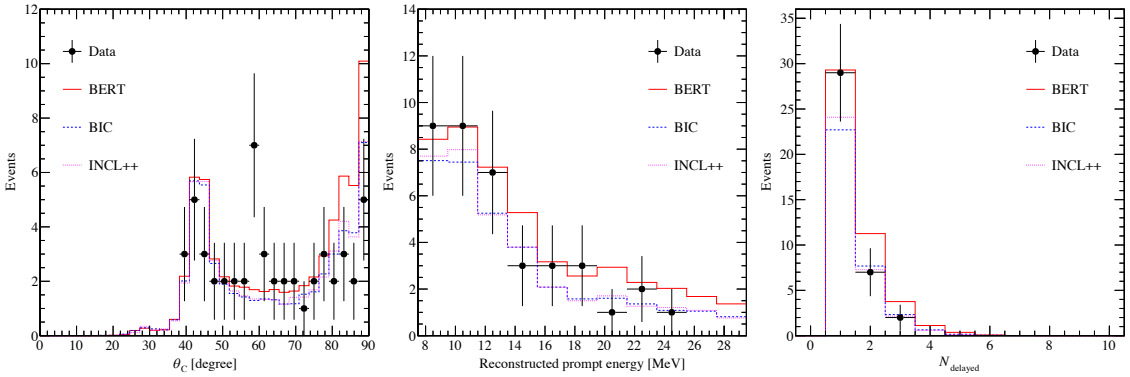

Figure 2: The distributions of θ_C (left), the reconstructed prompt energy (center) and N_{delayed} (right). In all distributions, the reconstructed prompt energy is between 7.5 MeV and 29.5 MeV, and N_{delayed} is greater or equal to one. The θ_C cut is not applied in θ_C distribution only.

The distributions of θ_C, the reconstructed prompt energy and N_{delayed} depend on the number of de-excitation gamma-rays and neutrons. For example, the direction of Cherenkov photons becomes more isotropic as the number of de-excitation gamma-rays becomes larger. Moreover, total energy of de-excitation gamma-rays is correlated to the number of de-excitation gamma-rays. Therefore, θ_C and the reconstructed prompt energy become larger as the number of de-excitaion gamma-rays becomes larger. Furthermore, naturally, N_{delayed} is correlated to the number of neutrons. By confirming these distributions, we can understand the property of each secondary interaction model.

This time, we use three secondary interaction models: BERT, BIC and INCL++, which are used for neutrons with hundreds of MeV. The distributions of θ_C, the reconstructed prompt energy and N_{delayed} in each model are shown in Fig. 2. The largest difference among the three models is the number of de-excitation gamma-rays and neutrons by secondary interactions. The trend of the number of de-excitation gamma-rays and neutrons is similar between BIC and INCL++. On the other hand, in BERT, the number of de-excitation gamma-rays and neutrons is larger than other two models. As a result, especially, the expected number of NCQE events and NC non-QE events becomes larger in BERT than other two models.

To judge which model is close to the observed data, we calculated χ^2 that defined as

$$\chi^2 = \sum_{i=1}^{\text{bin}} \left(\frac{N^{\text{obs},i} - N^{\text{exp},i}}{\delta N^{\text{obs},i}} \right)^2, \tag{6}$$

where bin is the number of bins that the observed number of events is not zero and $\delta N^{\text{obs},i}$ is the statistical uncertainty of i-th bin. χ^2 of θ_C is 25.479, 13.290 and 13.399 in BERT, BIC and INCL++, respectively. χ^2 of the reconstructed prompt energy is 6.693, 2.696 and 2.839 in BERT, BIC and INCL++, respectively. χ^2 of N_{delayed} is 4.138, 1.487 and 0.852 in BERT, BIC and INCL++, respectively. Due to the large statistical uncertainty, no significant difference was seen. However, as far as we see χ^2, we understood that BIC and INCL++ are closer to the observed data and established the verification method for secondary interaction models.

6. Conclusion and future prospects

We performed the first measurement of the NCQE cross section using atmospheric neutrinos in the SK-Gd experiment. 38 events were remained after applying event selections to 552.2 days of SK-VI data. The NCQE cross section was measured to be $0.74 \pm 0.22(\text{stat.})\,^{+0.86}_{-0.16}(\text{syst.}) \times 10^{-38}$ cm^2, which is consistent with the theoretical NCQE cross section and previous study. Furthermore, we established the verification method for secondary interaction models using atmospheric neutrino events and suggested that BIC and INCL++ are closer to the observed data.

The NCQE cross section measurement and the model verification using accelerator neutrinos have not yet been performed in SK-Gd phase. By performing the T2K experiment in SK-Gd phase, the statistics will increase, and the precision of the NCQE cross section measurement and the model verification will increase.

References

[1] J.F. Beacom and M.R. Vagins, *Antineutrino Spectroscopy with Large Water Čerenkov Detectors*, *Phys. Rev. Lett.* **93** (2004) 171101.

[2] M. Harada *et al.*, *Search for Astrophysical Electron Antineutrinos in Super-Kamiokande with 0.01% Gadolinium-loaded Water*, *Astrophys. J. Lett.* **951** (2023) L27.

[3] L. Wan *et al.*, *Measurement of the neutrino-oxygen neutral-current quasielastic cross section using atmospheric neutrinos at Super-Kamiokande*, *Phys. Rev. D* **99** (2019) 032005.

[4] S. Fukuda *et al.*, *The Super-Kamiokande detector*, *Nucl. Instrum. Methods Phys. Res., Sect. A* **501** (2003) 418.

[5] M. Honda *et al.*, *Improvement of low energy atmospheric neutrino flux calculation using the JAM nuclear interaction model*, *Phys. Rev. D* **83** (2011) 123001.

[6] E. Richard *et al.*, *Measurements of the atmospheric neutrino flux by Super-Kamiokande: Energy spectra, geomagnetic effects, and solar modulation*, *Phys. Rev. D* **94** (2016) 052001.

[7] Y. Hayato and L. Pickering, *The NEUT neutrino interaction simulation program library*, *Eur. Phys. J. Spec. Top.* **230** (2021) 4469.

[8] A. M. Ankowski *et al.*, *Analysis of γ-Ray Production in Neutral-Current Neutrino-Oxygen Interactions at Energies above 200 MeV*, *Phys. Rev. Lett.* **108** (2012) 052505.

[9] K. Abe *et al.*, *Measurement of the neutrino-oxygen neutral-current interaction cross section by observing nuclear deexcitation γ rays*, *Phys. Rev. D* **90** (2014) 072012.

[10] K. Abe *et al.*, *Measurement of neutrino and antineutrino neutral-current quasielasticlike interactions on oxygen by detecting nuclear deexcitation γ rays*, *Phys. Rev. D* **100** (2019) 112009.

[11] K. Abe *et al.*, *Diffuse supernova neutrino background search at Super-Kamiokande*, *Phys. Rev. D* **104** (2021) 122002.

Full Authors List: Super-Kamiokande Collaboration

K. Abe,[1,46] C. Bronner,[1] Y. Hayato,[1,46] K. Hiraide,[1,46] K. Hosokawa,[1] K. Ieki,[1,46] M. Ikeda,[1,46] J. Kameda,[1,46] Y. Kanemura,[1] R. Kaneshima,[1] Y. Kashiwagi,[1] Y. Kataoka,[1,46] S. Miki,[1] S. Mine,[1,6] M. Miura,[1,46] S. Moriyama,[1,46] Y. Nakano,[1] M. Nakahata,[1,46] S. Nakayama,[1,46] Y. Noguchi,[1] K. Sato,[1] H. Sekiya,[1,46] H. Shiba,[1] K. Shimizu,[1] M. Shiozawa,[1,46] Y. Sonoda,[1] Y. Suzuki,[1] A. Takeda,[1,46] Y. Takemoto,[1,46] H. Tanaka,[1,46] T. Yano,[1] S. Han,[2] T. Kajita,[2,46,22] K. Okumura,[2,46] T. Tashiro,[2] T. Tomiya,[2] X. Wang,[2] S. Yoshida,[2] P. Fernandez,[3] L. Labarga,[3] N. Ospina,[3] B. Zaldivar,[3] B. W. Pointon,[5,49] E. Kearns,[4,46] J. L. Raaf,[4] L. Wan,[4] T. Wester,[4] J. Bian,[6] N. J. Griskevich,[6] S. Locke,[6] M. B. Smy,[6,46] H. W. Sobel,[6,46] V. Takhistov,[6,24] A. Yankelevich,[6] J. Hill,[7] S. H. Lee,[8] D. H. Moon,[8] R. G. Park,[8] B. Bodur,[9] K. Scholberg,[9,46] C. W. Walter,[9,46] A. Beauchêne,[10] O. Drapier,[10] A. Giampaolo,[10] Th. A. Mueller,[10] A. D. Santos,[10] P. Paganini,[10] B. Quilain,[10] T. Nakamura,[11] J. S. Jang,[12] L. N. Machado,[13] J. G. Learned,[14] K. Choi,[15] N. Iovine,[15] S. Cao,[16] L. H. V. Anthony,[17] D. Martin,[17] N. W. Prouse,[17] M. Scott,[17] A. A. Sztuc,[17] Y. Uchida,[17] V. Berardi,[18] M. G. Catanesi,[18] E. Radicioni,[18] N. F. Calabria,[19] A. Langella,[19] G. De Rosa,[19] G. Collazuol,[20] F. Iacob,[20] M. Mattiazzi,[20] L. Ludovici,[21] M. Gonin,[22] G. Pronost,[22] C. Fujisawa,[23] Y. Maekawa,[23] Y. Nishimura,[23] R. Okazaki,[23] R. Akutsu,[24] M. Friend,[24] T. Hasegawa,[24] T. Ishida,[24] T. Kobayashi,[24] M. Jakkapu,[24] T. Matsubara,[24] T. Nakadaira,[24] K. Nakamura,[24,46] Y. Oyama,[24] K. Sakashita,[24] T. Sekiguchi,[24] T. Tsukamoto,[24] N. Bhuiyan,[25] G. T. Burton,[25] F. Di Lodovico,[25] J. Gao,[25] A. Goldsack,[25] T. Katori,[25] J. Migenda,[25] Z. Xie,[25] S. Zsoldos,[25,46] A. T. Suzuki,[26] Y. Takagi,[26] Y. Takeuchi,[26,46] J. Feng,[27] L. Feng,[27] J. R. Hu,[27] Z. Hu,[27] T. Kikawa,[27] M. Mori,[27] T. Nakaya,[27,46] R. A. Wendell,[27,46] K. Yasutome,[27] S. J. Jenkins,[28] N. McCauley,[28] P. Mehta,[28] A. Tarant,[28] Y. Fukuda,[29] Y. Itow,[30,31] H. Menjo,[30] K. Ninomiya,[30] J. Lagoda,[32] S. M. Lakshmi,[32] M. Mandal,[32] P. Mijakowski,[32] Y. S. Prabhu,[32] J. Zalipska,[32] M. Jia,[33] J. Jiang,[33] C. K. Jung,[33] M. J. Wilking,[33] C. Yanagisawa,[33,*] M. Harada,[34] Y. Hino,[34] H. Ishino,[34] Y. Koshio,[34,46] F. Nakanishi,[34] S. Sakai,[34] T. Tada,[34] T. Tano,[34] T. Ishizuka,[35] G. Barr,[36] D. Barrow,[36] L. Cook,[36,46] S. Samani,[36] D. Wark,[36,41] A. Holin,[37] F. Nova,[37] B. S. Yang,[38] J. Y. Yang,[38] J. Yoo,[38] J. E. P. Fannon,[39] L. Kneale,[39] M. Malek,[39] J. M. McElwee,[39] M. D. Thiesse,[39] L. F. Thompson,[39] S. T. Wilson,[39] H. Okazawa,[40] S. B. Kim,[42] E. Kwon,[42] J. W. Seo,[42] I. Yu,[42] A. K. Ichikawa,[43] K. D. Nakamura,[43] S. Tairafune,[43] K. Nishijima,[44] A. Eguchi,[45] K. Nakagiri,[45] Y. Nakajima,[45,46] S. Shima,[45] N. Taniuchi,[45] E. Watanabe,[45] M. Yokoyama,[45,46] P. de Perio,[46] S. Fujita,[46] K. Martens,[46] K. M. Tsui,[46] M. R. Vagins,[46,6] J. Xia,[46] S. Izumiyama,[47] M. Kuze,[47] R. Matsumoto,[47] M. Ishitsuka,[48] H. Ito,[48] Y. Ommura,[48] N. Shigeta,[48] M. Shinoki,[48] K. Yamauchi,[48] T. Yoshida,[48] R. Gaur,[49] V. Gousy-Leblanc,[49,†] M. Hartz,[49] A. Konaka,[49] X. Li,[49] S. Chen,[50] B. D. Xu,[50] B. Zhang,[50] M. Posiadala-Zezula,[51] S. B. Boyd,[52] R. Edwards,[52] D. Hadley,[52] M. Nicholson,[52] M. O'Flaherty,[52] B. Richards,[52] A. Ali,[53,49] B. Jamieson,[53] S. Amanai,[54] Ll. Marti,[54] A. Minamino,[54] and S. Suzuki[54]

[1]Kamioka Observatory, Institute for Cosmic Ray Research, University of Tokyo, Kamioka, Gifu 506-1205, Japan
[2]Research Center for Cosmic Neutrinos, Institute for Cosmic Ray Research, University of Tokyo, Kashiwa, Chiba 277-8582, Japan
[3]Department of Theoretical Physics, University Autonoma Madrid, 28049 Madrid, Spain
[4]Department of Physics, Boston University, Boston, MA 02215, USA
[5]Department of Physics, British Columbia Institute of Technology, Burnaby, BC, V5G 3H2, Canada
[6]Department of Physics and Astronomy, University of California, Irvine, Irvine, CA 92697-4575, USA
[7]Department of Physics, California State University, Dominguez Hills, Carson, CA 90747, USA
[8]Institute for Universe and Elementary Particles, Chonnam National University, Gwangju 61186, Korea
[9]Department of Physics, Duke University, Durham NC 27708, USA
[10]Ecole Polytechnique, IN2P3-CNRS, Laboratoire Leprince-Ringuet, F-91120 Palaiseau, France
[11]Department of Physics, Gifu University, Gifu, Gifu 501-1193, Japan
[12]GIST College, Gwangju Institute of Science and Technology, Gwangju 500-712, Korea
[13]School of Physics and Astronomy, University of Glasgow, Glasgow, Scotland, G12 8QQ, United Kingdom
[14]Department of Physics and Astronomy, University of Hawaii, Honolulu, HI 96822, USA
[15]Institute for Basic Science (IBS), Daejeon, 34126, Korea
[16]Institute For Interdisciplinary Research in Science and Education, ICISE, Quy Nhon, 55121, Vietnam
[17]Department of Physics, Imperial College London, London, SW7 2AZ, United Kingdom
[18]Dipartimento Interuniversitario di Fisica, INFN Sezione di Bari and Università e Politecnico di Bari, I-70125, Bari, Italy
[19]Dipartimento di Fisica, INFN Sezione di Napoli and Università di Napoli, I-80126, Napoli, Italy
[20]Dipartimento di Fisica, INFN Sezione di Padova and Università di Padova, I-35131, Padova, Italy
[21]INFN Sezione di Roma and Università di Roma "La Sapienza", I-00185, Roma, Italy
[22]ILANCE, CNRS - University of Tokyo International Research Laboratory, Kashiwa, Chiba 277-8582, Japan
[23]Department of Physics, Keio University, Yokohama, Kanagawa, 223-8522, Japan
[24]High Energy Accelerator Research Organization (KEK), Tsukuba, Ibaraki 305-0801, Japan
[25]Department of Physics, King's College London, London, WC2R 2LS, UK
[26]Department of Physics, Kobe University, Kobe, Hyogo 657-8501, Japan
[27]Department of Physics, Kyoto University, Kyoto, Kyoto 606-8502, Japan
[28]Department of Physics, University of Liverpool, Liverpool, L69 7ZE, United Kingdom
[29]Department of Physics, Miyagi University of Education, Sendai, Miyagi 980-0845, Japan

[*]also at BMCC/CUNY, Science Department, New York, New York, 1007, USA.
[†]also at University of Victoria, Department of Physics and Astronomy, PO Box 1700 STN CSC, Victoria, BC V8W 2Y2, Canada.

[30]Institute for Space-Earth Environmental Research, Nagoya University, Nagoya, Aichi 464-8602, Japan
[31]Kobayashi-Maskawa Institute for the Origin of Particles and the Universe, Nagoya University, Nagoya, Aichi 464-8602, Japan
[32]National Centre For Nuclear Research, 02-093 Warsaw, Poland
[33]Department of Physics and Astronomy, State University of New York at Stony Brook, NY 11794-3800, USA
[34]Department of Physics, Okayama University, Okayama, Okayama 700-8530, Japan
[35]Media Communication Center, Osaka Electro-Communication University, Neyagawa, Osaka, 572-8530, Japan
[36]Department of Physics, Oxford University, Oxford, OX1 3PU, United Kingdom
[37]Rutherford Appleton Laboratory, Harwell, Oxford, OX11 0QX, UK
[38]Department of Physics, Seoul National University, Seoul 151-742, Korea
[39]Department of Physics and Astronomy, University of Sheffield, S3 7RH, Sheffield, United Kingdom
[40]Department of Informatics in Social Welfare, Shizuoka University of Welfare, Yaizu, Shizuoka, 425-8611, Japan
[41]STFC, Rutherford Appleton Laboratory, Harwell Oxford, and Daresbury Laboratory, Warrington, OX11 0QX, United Kingdom
[42]Department of Physics, Sungkyunkwan University, Suwon 440-746, Korea
[43]Department of Physics, Faculty of Science, Tohoku University, Sendai, Miyagi, 980-8578, Japan
[44]Department of Physics, Tokai University, Hiratsuka, Kanagawa 259-1292, Japan
[45]Department of Physics, University of Tokyo, Bunkyo, Tokyo 113-0033, Japan
[46]Kavli Institute for the Physics and Mathematics of the Universe (WPI), The University of Tokyo Institutes for Advanced Study, University of Tokyo, Kashiwa, Chiba 277-8583, Japan
[47]Department of Physics,Tokyo Institute of Technology, Meguro, Tokyo 152-8551, Japan
[48]Department of Physics, Faculty of Science and Technology, Tokyo University of Science, Noda, Chiba 278-8510, Japan
[49]TRIUMF, 4004 Wesbrook Mall, Vancouver, BC, V6T2A3, Canada
[50]Department of Engineering Physics, Tsinghua University, Beijing, 100084, China
[51]Faculty of Physics, University of Warsaw, Warsaw, 02-093, Poland
[52]Department of Physics, University of Warwick, Coventry, CV4 7AL, UK
[53]Department of Physics, University of Winnipeg, MB R3J 3L8, Canada
[54]Department of Physics, Yokohama National University, Yokohama, Kanagawa, 240-8501, Japan

PoS(ICRC2023)1088